

# Nasomaxillary Expansion by Endoscopically-Assisted Surgical Expansion (EASE): An airway centric approach

Kasey LI<sup>1\*</sup>, Tomonori IWASAKI<sup>2</sup>, Stacey QUO<sup>3</sup>, Eileen B. LEARY<sup>4</sup>, Connor LI<sup>1</sup>, Christian GUILLEMINAULT<sup>5</sup>

<sup>1</sup> Sleep Apnea Surgery Center, 1900 University Avenue, Suite 105, East Palo Alto, CA, USA

<sup>2</sup> Developmental Medicine, Health Research Course, Graduate School of Medical and Dental Sciences, Kagoshima University, 8-35-1 Sakuragaoka, Kagoshima 890-8544, Japan

<sup>3</sup> School of Dentistry, University of California San Francisco, 707 Parnassus Ave, San Francisco, CA 94143, USA

<sup>4</sup> Center for Sleep Sciences and Medicine, Stanford University School of Medicine, Stanford, 3165 Porter Dr, Palo Alto, CA 94304, USA

<sup>5</sup> Deceased. Formally Sleep Medicine Division, Stanford University School of Medicine, Stanford, 3165 Porter Dr, Palo Alto, CA 94304, USA

## KEYWORDS:

OSA / EASE /

TPD / SARPE /

RPE / RME /

MARPE /

Maxillary expansion /

Nasomaxillary expansion

**ABSTRACT – Introduction:** *The aim of this study was to analyze the skeletal, dental and airway changes with endoscopically assisted surgical expansion (EASE) to widen the nasomaxillary complex for the treatment of sleep apnea in adults.* **Methods:** *One hundred and five consecutive patients underwent EASE. Cone beam computed tomography (CBCT) was conducted preoperatively and within four weeks after the completion of the expansion process. Computational fluid dynamic (CFD) analysis was performed on 20 randomly selected patients to assess airway flow changes.* **Results:** *One hundred patients (67 males) with the mean age of 35.0±13.5 years (17–64 years) had completed pre- and post-expansion imaging. Ninety-six patients (96%) had successful expansion defined as separation of the midpalatal suture at least 1 mm from anterior nasal spine (ANS) to posterior nasal spine (PNS). The nasal cavity expansion was 3.12±1.11 mm at ANS, 3.64±1.06 mm at first molar and 2.39±1.15 mm at PNS. The zygoma expansion was 2.17±1.11 mm. The ratio of dental expansion to skeletal expansion was 1.23:1 (3.83 mm:3.12 mm) at canine and 1.31:1 (4.77 mm:3.64 mm) at first molar. CFD airway simulation showed a dynamic change following expansion throughout the airway. The mean negative pressure improved in the nasal airway (from -395.5±721.0 to -32.7±19.2 Pa), nasopharyngeal airway (from -394.2±719.4 to -33.6±18.5 Pa), oropharyngeal airway (from -405.9±710.8 to -39.4±19.3 Pa) and hypopharyngeal airway (from -422.6±704.9 to -55.1±33.7 Pa). The mean airflow velocity within the nasal airway decreased from 18.8±15.9 to 7.6±2.0 m/s and the oropharyngeal airway decreased from 4.2±2.9 to 3.2±1.2 m/s. The velocity did not change significantly in the nasopharyngeal and hypopharyngeal regions.* **Conclusions:** *EASE results in expansion of the midpalatal suture from the ANS to PNS with a nearly pure skeletal movement of minimal dental effect. The expansion of the nasomaxillary complex resulted in the widening of the nasal sidewall throughout the nasal cavity. The improved air flow dynamics was demonstrated by CFD simulation.*

## 1. Introduction

Maxillary expansion is usually performed for the treatment of crossbite due to transverse maxillary deficiency. The use of maxillary expansion to treat obstructive sleep apnea syndrome (OSA) was first reported in 1998 in children and adults<sup>5</sup>. Over the past 20 years, numerous studies have documented the improvement of OSA with rapid palatal expansion (RPE) in children and surgically assisted rapid palatal expansion (SARPE) in adults<sup>3,12,26,28,31,32</sup>. The need of surgically assisted expansion approach in non-growing patients is justified due to the increased resistance to suture separation<sup>25</sup>. However, the expansion pattern between RPE and SARPE is different. RPE leads to a triangular opening in the frontal alveolar area where the apex of the expansion involves the nasal frontal suture<sup>6</sup>, thus resulting in enlargement of the entire nasal vault. SARPE on the other hand, primarily widens the lower portion maxilla due to the Le Fort I osteotomy. By design, SARPE widens the maxillary alveolus and the nasal floor while exerting less impact on the nasal airway above the osteotomy, thus limiting the extent of the airway impact (Fig. 1).

Mini-screw assisted rapid palatal expansion (MARPE) has been advocated in recent years to achieve a greater skeletal expansion with improved skeletal anchorage. The expansion pattern of MARPE has been shown to involve the entire zygomaxillary complex<sup>4,22,23,29</sup>, thus conceptually achieves a favorable expansion pattern when compared to SARPE (Fig. 1). However, the application of MARPE is primarily limited to teens and young adults. A systematic review of 264 MARPE patients showed an average age 12.3 years<sup>17</sup>. Additionally, although MARPE achieves a greater midpalatal suture opening as compared to conventional tooth-borne expanders, teeth tipping and dentoalveolar remains and the dental expansion still occurs in a considerably greater extent than skeletal expansion<sup>17,20,23</sup>.

To apply maxillary expansion as a treatment for OSA to all adults, a surgical procedure named endoscopically-assisted surgical expansion (EASE) was developed in 2017<sup>18</sup>. The operation was designed as a minimally invasive procedure to create a favorable nasomaxillary expansion pattern by maximizing airway improvement while limiting teeth inclination and dentoalveolar expansion. Initial results demonstrated reduction of OSA severity along with improvement of subjective symptoms<sup>18</sup>. The aim of this

study was to evaluate the skeletal, dental and airway changes with EASE based on cone beam computed tomography (CBCT) and computational fluid dynamics (CFD) analysis.

## 2. Materials and Methods

The data from one hundred and five consecutive patients that underwent EASE for the treatment of OSA were retrospectively reviewed. CBCT was conducted preoperatively and within four weeks after the completion of the expansion process. Additionally, CFD analysis was performed on 20 randomly selected patients to assess airway flow changes. This study was approved by IRB.

### 2.1. Surgical Procedure: endoscopically-assisted surgical expansion (EASE)

Surgery was performed by the same surgeon for all patients under either general anesthesia via oroendotracheal intubation or intravenous sedation. A small incision just behind the posterior tuberosity was made, and the pterygomaxillary suture was identified using a periosteal elevator. Gentle pterygomaxillary separation was achieved with a piezoelectric blade (DePuy Synthes, Switzerland). With the help of a nasal endoscope to visualize the nasal airway, a partial osteotomy was performed at the junction of the nasal septum and the nasal floor with the blade angled towards the midpalatal suture (Fig. 2). The depth of the osteotomy was planned based on the preoperative CBCT measurement. The osteotomy was performed bilaterally from the posterior nasal spine (PNS) to the greater palatine foramen (along the nasal floor). The ANS separation was achieved using a very thin osteotome via a stab incision between the maxillary incisors. A transpalatal distractor (TPD, KLS Martin Group, Jacksonville, FL) was inserted onto the palate at the region of the second premolar and the first molar. The TPD was fully engaged to the palatal bone and the foot plates of the TPD were stabilized with a 5 mm screw.

### 2.2. Expansion Process

The TPD was activated between 3 to 5 days after surgery by 0.1 to 0.3 mm per day. The expansion process is deemed complete when either the patient has experienced no further clinical improvement with continual expansion or when excessive buccal crossbite is present. Once expansion was completed,

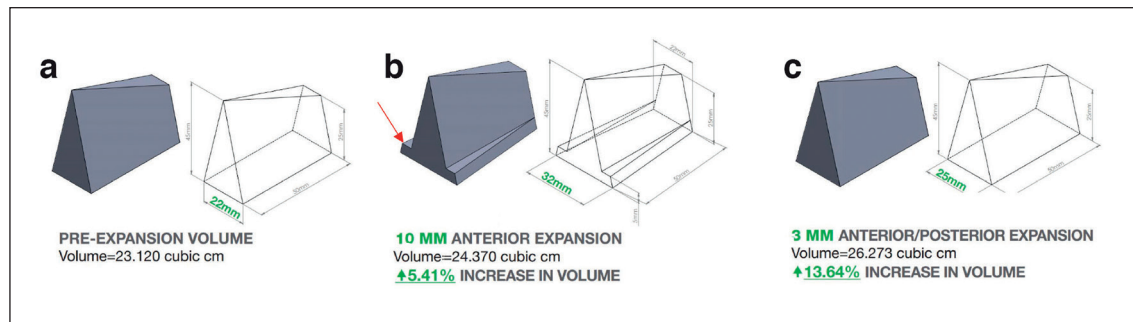


Figure 1

Solid modeling computer-aided design with SolidWorks®. (a) Hypothetical baseline nasal dimension. (b) Proposed 10 mm SARPE expansion pattern below the osteotomy (red arrow) without opening posteriorly. (c) Proposed 3 mm expansion with opening of the midpalatal suture anteriorly and posteriorly.

the TPD was locked and removed under local anesthesia three months later. Orthodontic treatment was initiated after the removal of the TPD.

### 2.3. Cone Beam Computed Tomography (CBCT)

All patients underwent CBCT preoperatively and within four weeks after the completion of the expansion. CBCT scans were acquired in the supine position in extended field modus (FOV: 16x22 cm, scanning time 2x20 s, voxel size 0.4 mm, NewTom 3D VGI, Cefla North America, Charlotte, NC). Data from CBCT were exported in Digital Imaging and communications in Medicine (DICOM) format into InVivo5® software (Anatomage, San Jose, CA, USA) and were reoriented with the palatal plane parallel to the floor in the sagittal and coronal planes. The following measurements were recorded by dental radiology technicians blinded to the study: intercanine width, nasal width at canine, intermolar width, nasal sidewall width at first molar, nasal sidewall width at posterior nasal spine and zygomatic width (Fig. 3).

### 2.4. Simulation of Airway Ventilation with Computational Fluid Dynamics (CFD)

Volume-rendering software (INTAGE Volume Editor, CYBERNET, Tokyo, Japan) was used to generate 3D volume data for the upper airway. Using mesh-morphing software (DEP Mesh Works/Morpher, IDAJ, Kobe, Japan), the 3D models were subsequently converted to a smoothed model without losing the patient-specific shape of the airway. CFD was used to simulate ventilation of the upper airway models (Fig. 4)<sup>14,15</sup>. The models were exported to fluid dynamics software (PHOENICS,

CHAM-Japan, Tokyo, Japan) in stereolithographic format, and the fluid was assumed to be Newtonian, homogeneous, and incompressible. Elliptic-staggered equations and a continuity equation were used in the analysis. The CFD of the upper airway models was analyzed under the following conditions: volumetric flow rate of 7 ml/s/kg no-slip condition at the wall surface, and 300 iterations to calculate mean values. Convergence was judged by monitoring the magnitude of the absolute residual sources of mass and momentum, normalized to their respective inlet fluxes. The iteration was continued until all residuals fell below 0.2%. Simulation of estimated airflow pressure and velocity was performed at the nasal airway, nasopharyngeal airway (NA), oropharyngeal airway (OA), and hypopharyngeal airway (HA).

### 2.5. Statistical Analyses

Descriptive statistics and frequency distributions were performed on demographic and surgical characteristics. Means and standard deviations are reported for continuous variables, and number and percent for categorical variables. Data were evaluated for extreme or implausible values and missingness. The paired student's t-test was used to compare mean of the differences between the preoperative and postoperative samples. Difference in means was reported with 95% confidence interval. For the CFD data, the paired sample Wilcoxon signed-rank test was used due to the small sample size and skewed distribution of some measures. Analyses were performed using R Studio Version 1.1.463. A 2-sided p-value < 0.05 was used to indicate statistical significance.



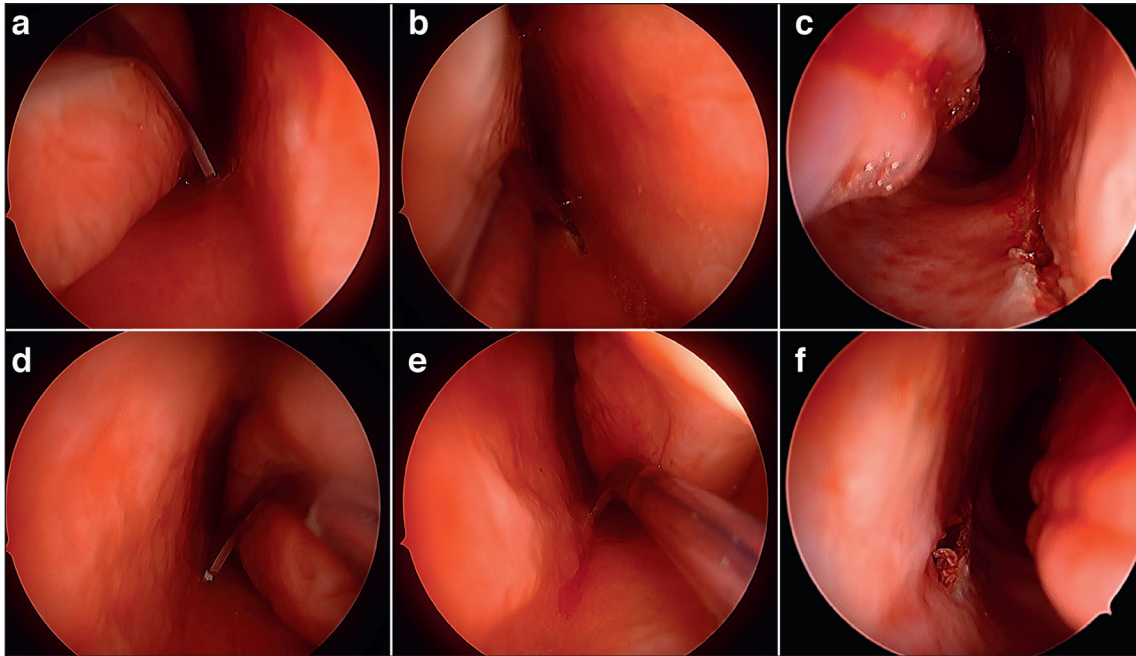


Figure 2

EASE procedure. (a) Piezoelectric blade at PNS in the right nasal cavity. (b) Osteotomy from the PNS. (c) Osteotomy completed. (d) Piezoelectric blade at the PNS in the left nasal cavity. (e) Osteotomy from the PNS. (f) Osteotomy completed.

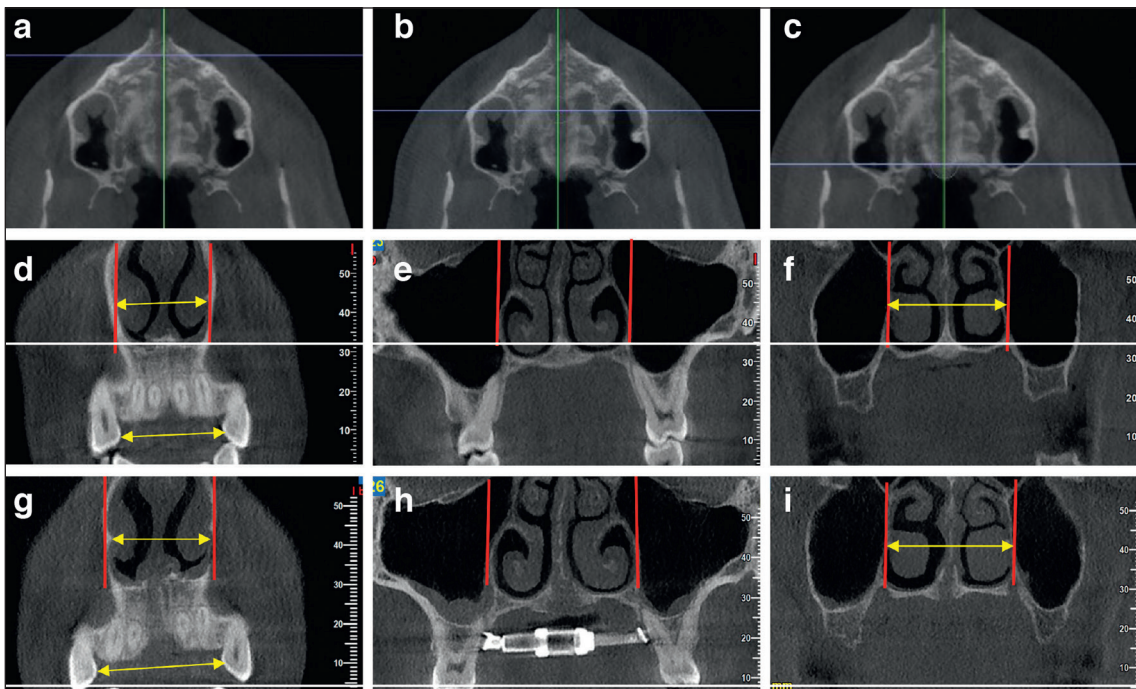


Figure 3

CBCT measurements. (a) Location of anterior measurement at canine. (b) Location of measurement at first molar. (c) Location of posterior measurement at PNS. (d) Frontal view of preoperative intercanine width and nasal width measurement. (e) Frontal view of preoperative intermolar width and nasal width measurement. (f) Frontal view of preoperative nasal width measurement at PNS. (g) Frontal view of postoperative intercanine width and nasal width measurement. (h) Frontal view of postoperative intermolar width and nasal width measurement. (i) Frontal view of postoperative nasal width measurement at PNS.

### 3. Results

One hundred and five consecutive patients underwent EASE. Five patients did not undergo post-expansion CBCT and were excluded from the analysis. One hundred patients (67 males) with the mean age of  $35.0 \pm 13.5$  years (17-64 years) had completed pre- and post-expansion imaging (Tables 1 and 2). Ninety-six patients (96%) had successful expansion defined as separation of the midpalatal suture at least 1 mm from anterior nasal spine (ANS) to posterior nasal spine (PNS). Two patients had separation of the ANS but not PNS and two patients did not have separation of the midpalatal suture. The nasal sidewall expansion was  $3.12 \pm 1.11$  mm at canine,  $3.64 \pm 1.06$  mm at first molar and  $2.39 \pm 1.15$  mm at PNS. The zygoma expansion was  $2.17 \pm 1.11$  mm. The ratio of dental expansion to skeletal expansion was 1.23:1 ( $3.83$  mm: $3.12$  mm) at canine and 1.31:1 ( $4.77$  mm: $3.64$  mm) at first molar. Ninety-six patients (96%) had a near parallel expansion pattern with opening of the ANS to PNS (Figs. 5 to 10).

CFD simulation was performed on 20 randomly selected patients (Table 1) to assess airway flow changes (Table 3). The mean airflow velocity within the nasal airway changed from  $18.8 \pm 15.9$  to  $7.6 \pm 2.0$  m/s and the oropharyngeal airway decreased from  $4.2 \pm 2.9$  to  $3.2 \pm 1.2$  m/s. The airflow velocity did not significantly change in the nasopharyngeal airway (from  $3.0 \pm 3.1$  to  $2.2 \pm 1.1$  m/s) or the hypo-

pharyngeal airway (from  $3.9 \pm 1.6$  to  $3.8 \pm 1.7$  m/s). The mean negative pressure improved in the nasal airway (from  $-395.5 \pm 721.0$  to  $-32.7 \pm 19.2$  Pa), nasopharyngeal airway (from  $-394.2 \pm 719.4$  to  $-33.6 \pm 18.5$  Pa), oropharyngeal airway (from  $-405.9 \pm 710.8$  to  $-39.4 \pm 19.3$  Pa) and hypopharyngeal airway (from  $-422.6 \pm 704.9$  to  $-55.1 \pm 33.7$  Pa).

### 4. Discussion

The nose is the most resistive element of the airway that accounts for 50% of the total airway resistance<sup>11,27</sup>. Hence, the objective of maxillary expansion is to maximize the enlargement of the nasal airway to diminish the resistance of nasal airflow. In an attempt to maximize nasal widening by SARPE, modified SARPE such as distraction osteogenesis maxillary expansion (DOME) has been advocated. DOME incorporated the use of mini-screws to improve skeletal anchorage along with over-widening of the maxilla (10+mm) in treating OSA patients<sup>21,35</sup>. However, the pattern of expansion remains the same for all forms of SARPE because Le Fort I osteotomy is incorporated. Moreover, excessive widening can lead to lack of bone fill in the maxillary alveolus and devitalization of the teeth thus resulting in long-term problems<sup>19</sup>. Indeed, severe complications related to SARPE, including loss of bone and teeth, have been previously reported<sup>9,23</sup>.

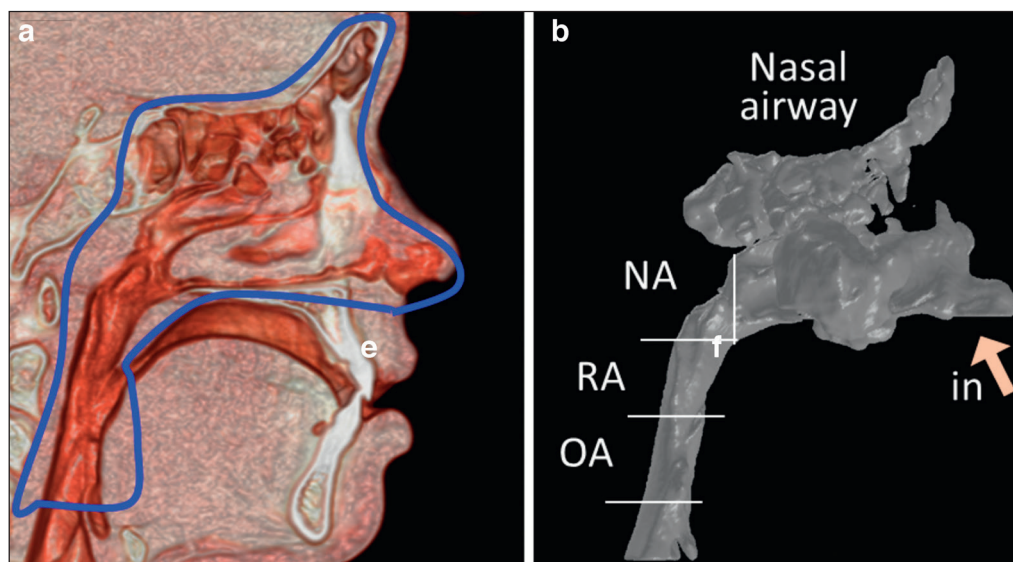


Figure 4

Evaluation of upper airway ventilation using computed fluid dynamics. (a) Extraction of the upper airway. (b) Construction of three-dimensional upper airway model and numeric simulation (inspiration air mass flow: 7 ml/s/kg), at nasopharynx (NA), oropharynx (RA) and hypopharynx (OA).



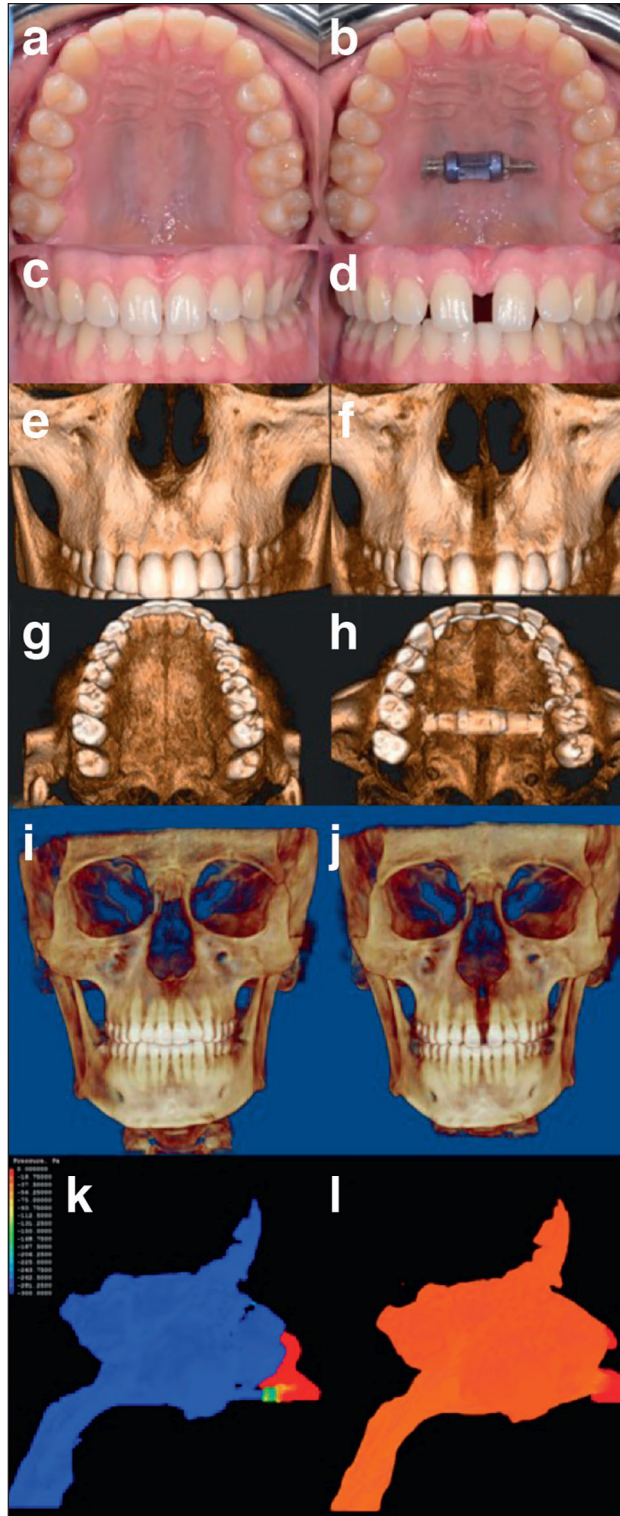


Figure 5

21-year-old patient's expansion photos, CBCT and CFD images. (a) Preoperative palatal view. (b) Postoperative palatal view showing the TPD in place at the completion of expansion. (c) Preoperative frontal view. (d) Postoperative frontal view. (e) Preoperative frontal view. (f) Postoperative frontal view at the completion of expansion showing widening at ANS. (g) Preoperative palatal view. (h) Postoperative palatal showing a parallel expansion at the mid-palatal suture from ANS to PNS. (i) Preoperative frontal skull view. (j) Postoperative frontal skull view showing the expanded maxilla. Note the widening between the roots of the central incisors with minimal to no teeth tipping, expanded nasal aperture and modulation of the sutures at the nasofrontal region. (k) CFD showing preoperative airway pressures. (l) CFD showing postoperative airway pressures.

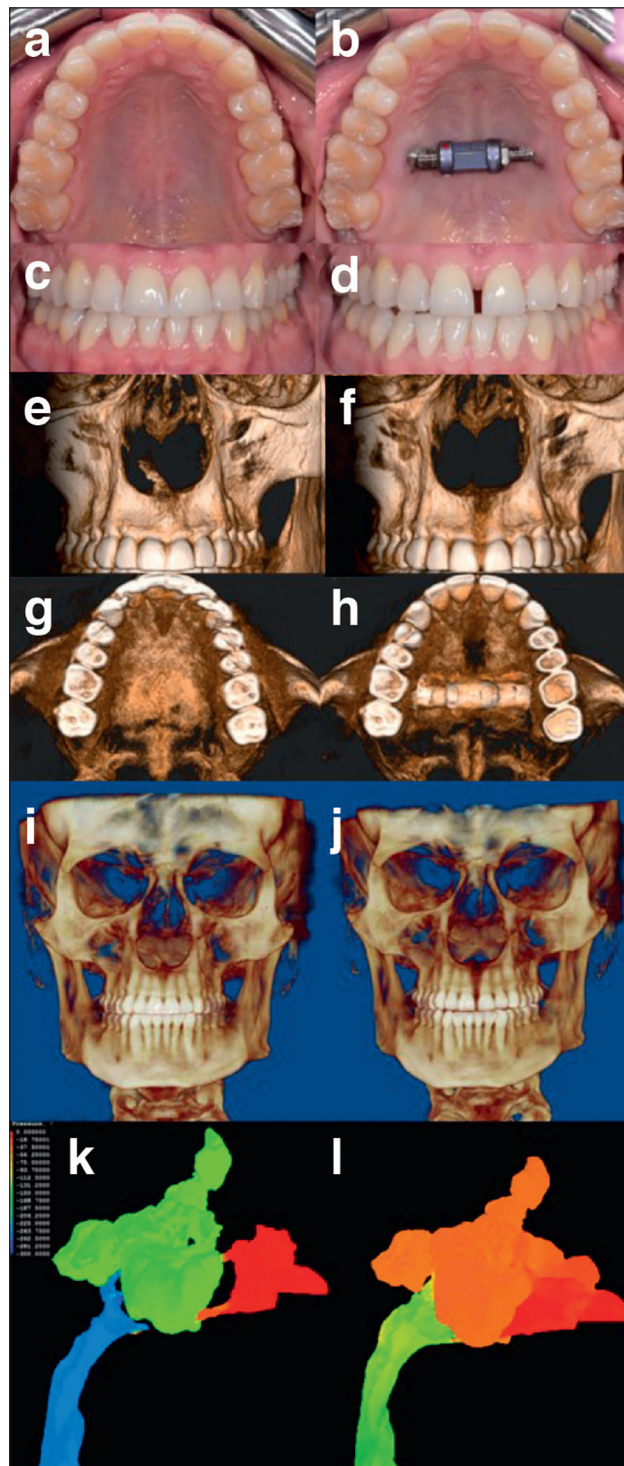


Figure 6

28-year-old patient's expansion photos, CBCT and CFD images. (a) Preoperative palatal view. (b) Postoperative palatal view showing the TPD in place at the completion of expansion. (c) Preoperative frontal view. (d) Postoperative frontal view. (e) Preoperative frontal view. (f) Postoperative frontal view at the completion of expansion showing widening at ANS. (g) Preoperative palatal view. (h) Postoperative palatal showing a parallel expansion at the mid-palatal suture from ANS to PNS. (i) Preoperative frontal skull view. (j) Postoperative frontal skull view showing the expanded maxilla. Note the widening between the roots of the central incisors with minimal to no teeth tipping, expanded nasal aperture and modulation of the sutures at the nasofrontal region. (k) CFD showing preoperative airway pressures. (l) CFD showing postoperative airway pressures.

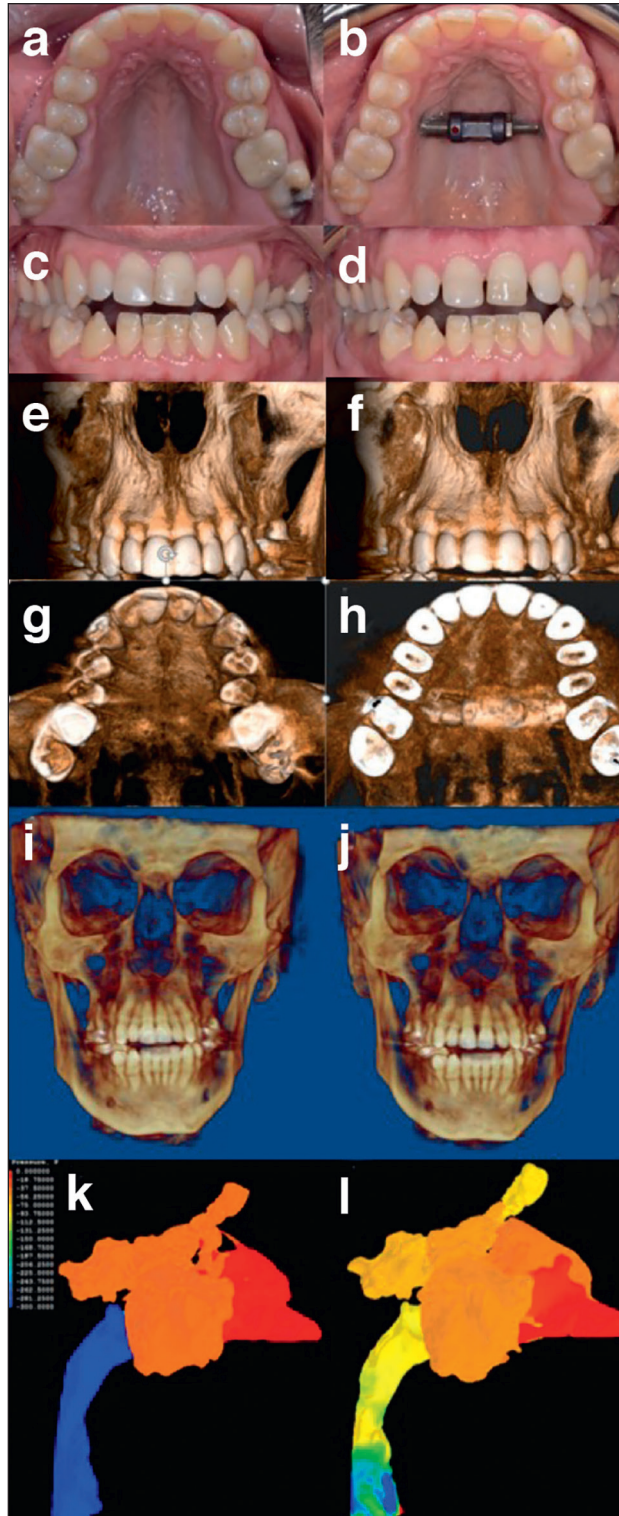


Figure 7

36-year-old patient's expansion photos, CBCT and CFD images. (a) Preoperative palatal view. (b) Postoperative palatal view showing the TPD in place at the completion of expansion. (c) Preoperative frontal view. (d) Postoperative frontal view. (e) Preoperative frontal view. (f) Postoperative frontal view at the completion of expansion showing widening at ANS. (g) Preoperative palatal view. (h) Postoperative palatal showing a parallel expansion at the mid-palatal suture from ANS to PNS. (i) Preoperative frontal skull view. (j) Postoperative frontal skull view showing the expanded maxilla. Note the widening between the roots of the central incisors with minimal to no teeth tipping, expanded nasal aperture and modulation of the sutures at the nasofrontal region. (k) CFD showing preoperative airway pressures. (l) CFD showing postoperative airway pressures.



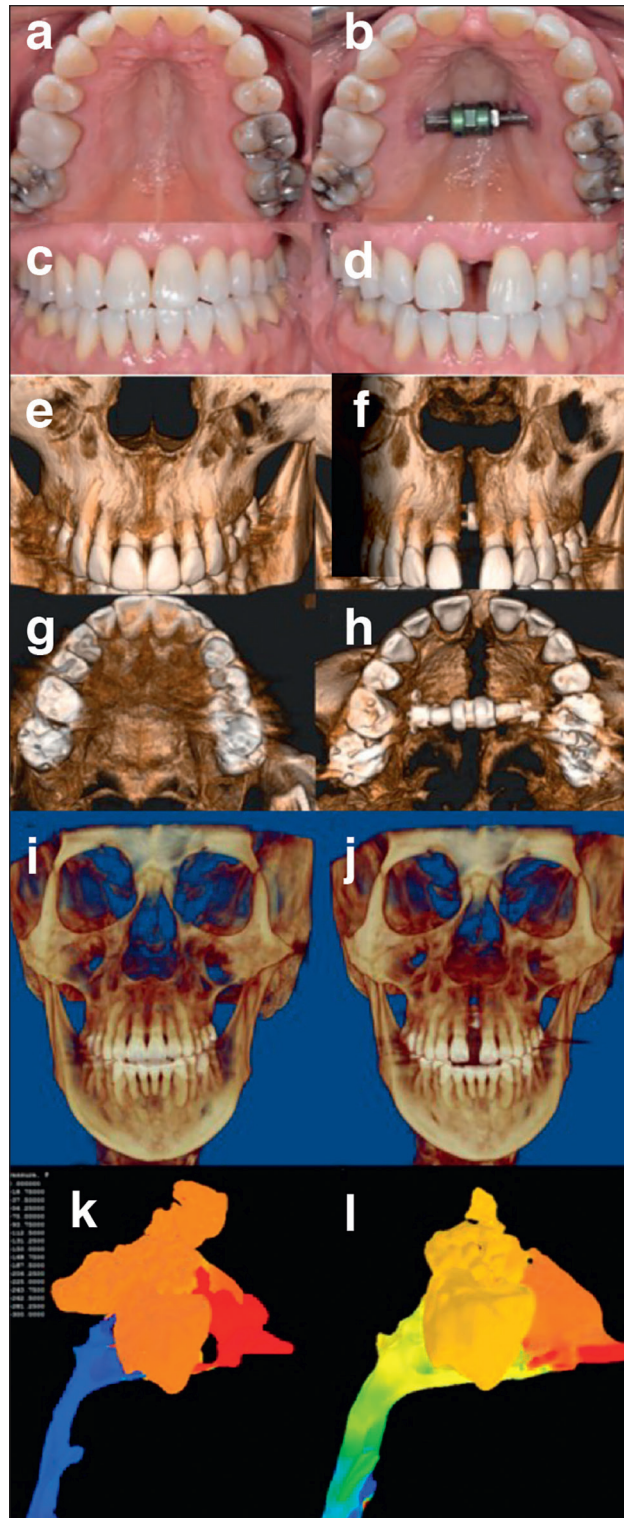


Figure 8

48-year-old patient's expansion photos, CBCT and CFD images. (a) Preoperative palatal view. (b) Postoperative palatal view showing the TPD in place at the completion of expansion. (c) Preoperative frontal view. (d) Postoperative frontal view. (e) Preoperative frontal view. (f) Postoperative frontal view at the completion of expansion showing widening at ANS. (g) Preoperative palatal view. (h) Postoperative palatal showing a parallel expansion at the mid-palatal suture from ANS to PNS. (i) Preoperative frontal skull view. (j) Postoperative frontal skull view showing the expanded maxilla. Note the widening between the roots of the central incisors with minimal to no teeth tipping, expanded nasal aperture and modulation of the sutures at the nasofrontal region. (k) CFD showing preoperative airway pressures. (l) CFD showing postoperative airway pressures.

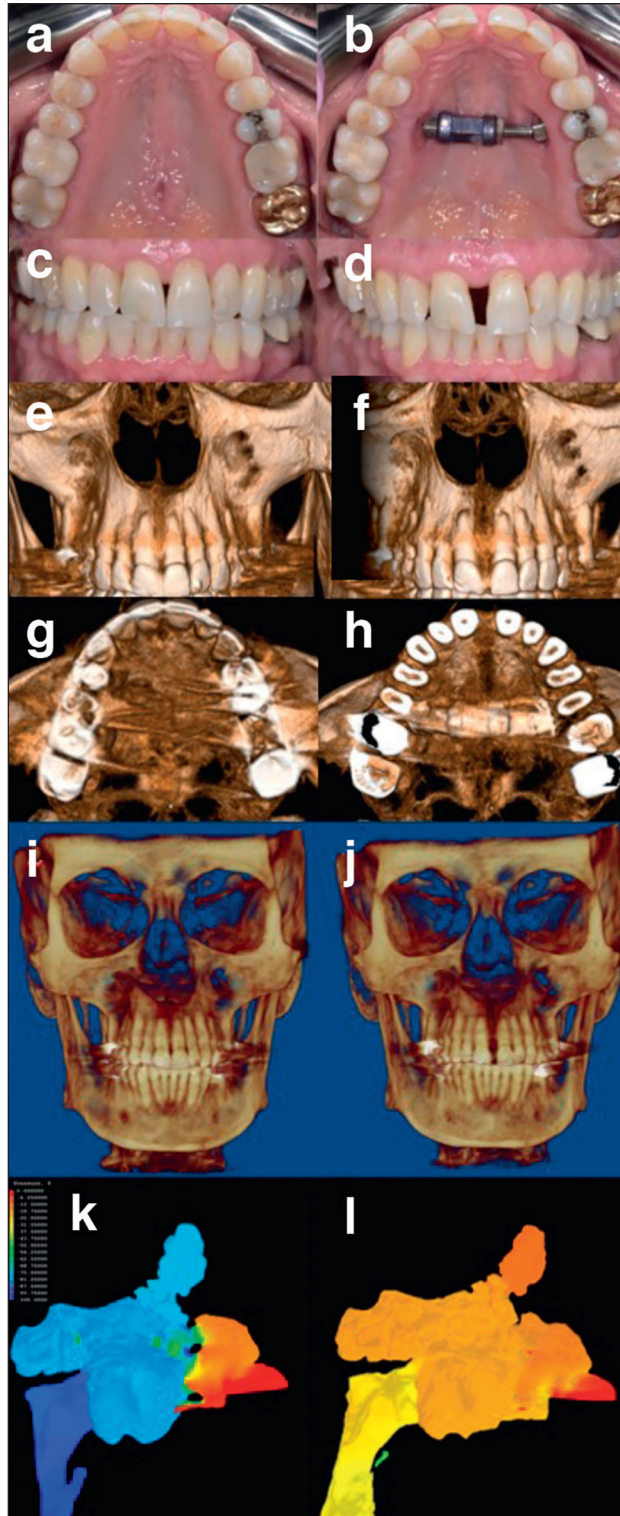


Figure 9

60-year-old patient's expansion photos, CBCT and CFD images. (a) Preoperative palatal view. (b) Postoperative palatal view showing the TPD in place at the completion of expansion. (c) Preoperative frontal view. (d) Postoperative frontal view. (e) Preoperative frontal view. (f) Postoperative frontal view at the completion of expansion showing widening at ANS. (g) Preoperative palatal view. (h) Postoperative palatal showing a parallel expansion at the mid-palatal suture from ANS to PNS. (i) Preoperative frontal skull view. (j) Postoperative frontal skull view showing the expanded maxilla. Note the widening between the roots of the central incisors with minimal to no teeth tipping, expanded nasal aperture and modulation of the sutures at the nasofrontal region. (k) CFD showing preoperative airway pressures. (l) CFD showing postoperative airway pressures.

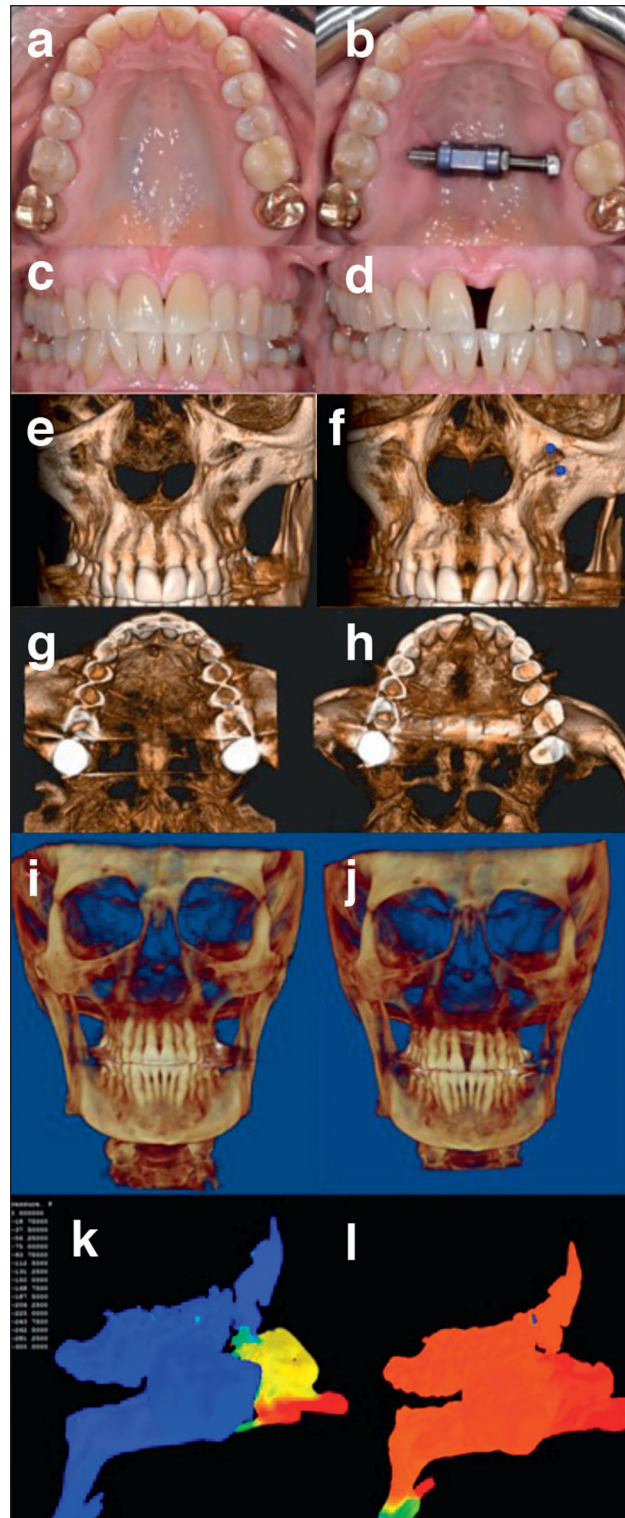


Figure 10

62-year-old patient's expansion photos, CBCT and CFD images. (a) Preoperative palatal view. (b) Postoperative palatal view showing the TPD in place at the completion of expansion. (c) Preoperative frontal view. (d) Postoperative frontal view. (e) Preoperative frontal view. (f) Postoperative frontal view at the completion of expansion showing widening at ANS. (g) Preoperative palatal view. (h) Postoperative palatal showing a parallel expansion at the mid-palatal suture from ANS to PNS. (i) Preoperative frontal skull view. (j) Postoperative frontal skull view showing the expanded maxilla. Note the widening between the roots of the central incisors with minimal to no teeth tipping, expanded nasal aperture and modulation of the sutures at the nasofrontal region. (k) CFD showing preoperative airway pressures. (l) CFD showing postoperative airway pressures.



Due to the increasing complications that we have observed with over-expansion from DOME, the EASE procedure was designed to maximize the nasal airway expansion while minimizing the undesired effects. EASE focuses on the entire nasomaxillary complex, including the posterior region of the maxilla, which has been shown to be the most resistant to expansion<sup>7,30</sup>. The minimal anterior surgical intervention also eliminates concerns of esthetic changes including nasal base widening and lip shortening<sup>1,10,13</sup>. The release of the pterygomaxillary suture and posterior midpalatal suture along with direct pressure applied at the palatal bone promoted the separation of the maxilla in the posterior aspect that propagated anteriorly while avoiding extensive surgical intervention in the anterior maxilla. The resultant parallel expansion pattern along the midpalatal suture was achieved consistently. Most importantly, the entire nasal cavity was enlarged with the expansion extended to the nasofrontal region as demonstrated by the widening of the zygoma width and the modulation of the sutures at the nasofrontal region (Figs. 5 to 10).

The ratio of dental expansion to skeletal expansion was 1.28:1 (4.1 mm:3.2 mm) at canine and 1.3:1 (4.7 mm:3.6 mm) at first molar. It is evident that the skeletal impact of EASE is considerably more efficient than other types of expansion methods, which is usually accepted as being approximately 3:1 even when MARPE is utilized in adolescent and young adults<sup>6,17,20,23</sup>. The skeletal impact of EASE is also considerably greater than SARPE, with a reported dental to skeletal expansion ratio of 2.1:1 (7.0 mm:3.3 mm) in a meta-analysis review<sup>2</sup>. The difference in nasal airway expansion is more

profound where SARPE expansion is primarily located at the alveolar region.

Furthermore, the skeletal effect achieved by EASE is even more impressive considering the mean age of the study group (35.0 years), which is the oldest study sample of maxillary expansion published to date. The results also showed that a nearly pure skeletal nasomaxillary expansion with expansion pattern simulating the pediatric pattern that extends to the nasofrontal sutures is realistic in middle age and beyond.

This is the first description of nasomaxillary expansion at both the anterior nasal cavity (at the nasal vestibule and nasal valves) along with expansion of the posterior nasal cavity (at the junction of the nasal airway to the nasopharyngeal region). Traditionally, the molar region has been reported as the posterior extent of the maxillary expansion. However, the first molar only represents the midway of the nasal cavity. EASE resulted in expansion of the nasal airway posterior to the first molar, including the PNS. This expansion pattern is quite different than the typical fan shape surgical expansion where nasal floor widening can be inconsistent or inadequate<sup>7,8,24</sup>. The lack of posterior midpalatal suture opening minimally impacts the posterior nasal airway and the posterior hard palate, where several palatopharyngeal muscles originate, which impacts the nasopharyngeal and retropalatal airway. Despite the near consistent expansion pattern achieved by EASE, we did find the opening isn't completely parallel, with variation of the skeletal widening of the nasal sidewall at canine (3.2 mm), molar (3.6 mm), and PNS (2.2 mm). This is likely related to the direct pressure applied at the palatal shelves near molar roots causing greater

**Table 1.** Baseline Demographic Characteristics of the Full Sample and the Computational Fluid Dynamics (CFD) Sub-sample.

Characteristics	Mean ± SD or Count (%)	
	Full Sample (n=100)	CFD Sample (n=20)
Age, years	35.0 ± 13.5	35.4 ± 14.6
Gender		
Male	67 (67.0 %)	15 (75.0 %)
Female	33 (33.0 %)	5 (25.0 %)
Body Mass Index (BMI)	23.5 ± 3.0	23.1 ± 2.7

Abbreviations: CFD = Computational Fluid Dynamics.

**Table 2.** Pre- and Post-operative Dental and Skeletal Expansion Outcomes.

Characteristics (n=100)	Preoperative Mean $\pm$ SD	Postoperative Mean $\pm$ SD	Difference (95% CI)	t (df=99)	p-value
<b>Dental Expansion</b>					
Inter canine width (mm)	24.36 $\pm$ 2.88	28.19 $\pm$ 2.98	3.83 (3.46 - 4.19)	20.77	<0.0001
Inter molar width (mm)	33.65 $\pm$ 3.07	38.42 $\pm$ 3.63	4.77 (4.44 - 5.10)	28.57	<0.0001
<b>Skeletal Expansion</b>					
Nasal anterior nasal spine width at canine (mm)	22.58 $\pm$ 2.20	25.70 $\pm$ 2.11	3.12 (2.90 - 3.34)	28.57	<0.0001
Nasal sidewall width at first molar (mm)	29.27 $\pm$ 2.88	32.91 $\pm$ 2.74	3.64 (3.43 - 3.84)	34.61	<0.0001
Nasal sidewall width at posterior nasal spine (mm)	29.20 $\pm$ 2.54	31.58 $\pm$ 2.58	2.39 (2.16 - 2.61)	21.05	<0.0001
Zygomatic width (mm)	108.74 $\pm$ 5.40	110.91 $\pm$ 5.82	2.17 (1.95 - 2.39)	19.88	<0.0001

Abbreviations: df = degrees of freedom, mm = millimeters.

alveolar bending/teeth tilting in the region as well as lesser resistance to expansion anteriorly and greater resistant to expansion posteriorly.

The impact of nasomaxillary expansion pattern achieved by EASE on airflow properties was modeled using CFD. CFD simulation showed a dynamic change following expansion in airway pressure and velocity not only in the nasal airway but also consistently affected the upper airway segments posterior to the nasal airway. We postulate that the reduction of nasal airway resistance from expansion led to lower airway velocity and reduced negative nasal pressure on inspiration, with subsequent impact on the rest of the airway. The effect rendered the compliant airway less collapsible to the negative intraluminal pressure on inspiration, thus leading to reduction of OSA severity<sup>18</sup>. A similar concept has previously been proposed in the CFD study in children with OSA<sup>34</sup>. The impact on airway negative pressure by EASE was shown to be greater than five times that of the DOME on CFD simulation<sup>16</sup>.

The major limitations of this study is that it is retrospective in nature and lacks a control group. However, because the objective of the study was to assess the skeletal changes comparing CBCT and CDF of preoperative and postoperative imagi-

nings, we believe this study design lends sufficient credibility to the results. Additionally, retrospective study design in evaluating maxillary expansion results based on imaging or dental casts has been commonly used. Further studies are needed to show the clinical benefit of the EASE procedure evaluating obstructive sleep apnea outcomes in a larger sample size with longer follow-up periods. While a study comparing EASE patients with a control group of untreated patients plus traditional SARPE patients may have been ideal, it was not feasible because we have abandoned the SARPE approach completely.

## 5. Conclusion

EASE is a surgical approach to expand the nasomaxillary region extending from the nasal floor to the nasofrontal region. It results in a near parallel expansion of the midpalatal suture from the ANS to PNS with an almost pure skeletal movement of minimal dental effect. The expansion of the nasomaxillary complex results in reduction of airway pressure and velocity in simulated airway study by CFD, which is postulated to improve airway collapse in OSA.

**Table 3.** Pre- and Post-operative Mean Airflow Velocity and Negative Pressure Outcomes Based on Simulation of Airway Ventilation with Computational Fluid Dynamics (CFD).

Characteristics (n=20)	Preoperative Mean $\pm$ SD	Postoperative Mean $\pm$ SD	Difference Mean $\pm$ SD	V	p-value
<b>Mean Airflow Velocity</b>					
Nasal airway (m/s)	18.78 $\pm$ 15.90	7.61 $\pm$ 1.95	-11.17 $\pm$ 37.45	1	p=0.0001
Nasopharyngeal airway (m/s)	3.00 $\pm$ 3.14	2.17 $\pm$ 1.09	-0.84 $\pm$ 8.27	85	p=0.47
Oropharyngeal airway (m/s)	4.15 $\pm$ 2.94	3.16 $\pm$ 1.22	-0.99 $\pm$ 6.12	40.5	p=0.05
Hypopharyngeal airway (m/s)	3.88 $\pm$ 1.58	3.75 $\pm$ 1.74	-0.13 $\pm$ 4.78	95	p=0.72
<b>Mean Negative Pressure</b>					
Nasal airway (Pa)	-395.46 $\pm$ 720.95	-32.65 $\pm$ 19.19	362.82 $\pm$ 1712.442	208	<0.0001
Nasopharyngeal airway (Pa)	-394.18 $\pm$ 719.38	-33.60 $\pm$ 18.51	360.58 $\pm$ 1711.64	205	<0.0001
Oropharyngeal airway (Pa)	-405.86 $\pm$ 710.82	-39.40 $\pm$ 19.32	366.46 $\pm$ 1687.96	207	<0.0001
Hypopharyngeal airway (Pa)	-422.57 $\pm$ 704.86	-55.06 $\pm$ 33.68	367.51 $\pm$ 1651.66	208	<0.0001

Abbreviations: m/s = meter per second, Pa = pascal, CFD = Computational Fluid Dynamics.

## Links of interest

The authors declare that they have no interest in the data published in this article.

## References

- Berger JL, Pangrazio-Kulbersh V, Thomas BW, *et al*. Radiographic analysis of facial changes associated with maxillary expansion. *Am J Orthod Dentofacial Orthop* 1999;116:563-571.
- Bortolotti F, Solidoro L, Bartolucci ML, Parenti PI, Paganelli C, Alessandri-Bonetti G. Skeletal and dental effects of surgically assisted rapid palatal expansion: A systematic review of randomized controlled trials. *Eur J Orthod* 2019;1:cjz057. Doi:10.1093/ejo/cjz057.
- Camacho M, Chang ET, Song SA, *et al*. Rapid maxillary expansion for pediatric obstructive sleep apnea: a systematic review and meta-analysis. *Laryngoscope* 2017;127:1712-1719.
- Cantarella D, Dominguez-Mompell R, Moschik C, Stogliano L, Elkenawy I, Pan HC, Mallya SM, Moon W. Zygomaticomaxillary modification in the horizontal plane induced by micro-implant-supported skeletal expander, analyzed with CBCT images. *Prog Orthod* 2018;19:41.
- Cistulli PA, Palmisano RG, Poole MD. Treatment of obstructive sleep apnea syndrome by rapid maxillary expansion. *Sleep* 1998;21:831-835.
- Da Silva Filho OG, Montes LA, Torelly LF. Rapid maxillary expansion in the deciduous and mixed dentition evaluated through posterior-anterior cephalometric analysis. *Am J Orthod* 1995;107:268-275.
- De Assis DS, Xavier TA, Noritomi PY, *et al*. Finite element analysis of bone stress after SARPE. *J Oral Maxillofac Surg* 2014;72:167.e1-7.
- Deeb W, Hansen L, Hotan T, *et al*. Changes in nasal volume after surgically assisted bone-borne rapid maxillary expansion. *Am J Orthod Dentofacial Orthop* 2010;137:782-789.
- Dergin G, Aktop S, Varol A, *et al*. Complications related to surgically assisted rapid palatal expansion. *Oral Surg Oral Med Oral Pathol Oral Radiol* 2015;119:601-607.
- Ferrario VFR, Sforza C, Schmitz JH, *et al*. Three-dimensional facial morphometric assessment of soft tissue changes after orthognathic surgery. *Oral Surg Oral Med Oral Pathol Oral Radiol Endod* 1999;88:549-556.
- Ferris BG Jr, Mead J, Opie LH. Partitioning of respiratory flow resistance in man. *J Appl Physiol* 1964;19:653-658.
- Guillemainault C, Li KK. Maxillomandibular expansion for the treatment of sleep-disordered breathing: preliminary result. *Laryngoscope* 2004;114:893-896.
- Herford AS, Akin L, Ciccio M. Maxillary vestibular incision for surgically assisted rapid palatal expansion: evidence for a conservative approach. *Orthodontics* 2012;13:168-175.
- Iwasaki T, Saitoh I, Takemoto Y, Inada E, Kanomi R, Hayasaki H, Yamasaki Y. Evaluation of upper airway obstruction in Class II children with fluid-mechanical simulation. *Am J Orthod Dentofacial Orthop* 2011;139(2):e135-145.
- Iwasaki T, Takemoto Y, Inada E, Sato H, Suga H, Saitoh I, Kakuno E, Kanomi R, Yamasaki Y. The effect of rapid maxillary expansion on pharyngeal airway pressure during inspiration evaluation using computational fluid dynamics. *Int J Pediatr Otorhinolaryngol* 2014;78:1258-1264.
- Iwasaki T, Yoon A, Guillemainault C, Yamasaki Y, Liu SY. How does distraction osteogenesis maxillary expansion (DOME) reduce severity of obstructive sleep apnea. *Sleep and Breathing* 2020;24:287-296.
- Krüsi M, Eliades T, Papageorgiou N. Are there benefits from using bone-borne maxillary expansion instead of tooth-borne maxillary expansion? A systematic review with meta-analysis. *Prog Orthod* 2019;20:9. Doi: 10.1186/s40510-019-0261-5.



18. Li KK, Quo S, Guilleminault C. Endoscopically-assisted surgical expansion (EASE) for the treatment of obstructive sleep apnea. *Sleep Med* 2019;60:53-59.
19. Li KK. Letter to the editor regarding "Distraction Osteogenesis Maxillary Expansion (DOME) for adult obstructive sleep apnea patients with narrow maxilla and nasal floor" by Yoon, *et al.* *Sleep Med* 2020;74:298-300.
20. Lim HM, Park YC, Lee KJ, Kim KH, Choi YJ. Stability of dental, alveolar, and skeletal changes after miniscrew-assisted rapid palatal expansion. *Korean J Orthod* 2017;47:313-322.
21. Liu SYC, Guilleminault C, Huon LK, Yoon A. Distraction osteogenesis maxillary expansion (DOME) for adult obstructive sleep apnea patients with high arched palate. *Otolaryngol Head Neck Surg* 2017;157:345-348.
22. MacGinnis M, Chu H, Youssef G, Wu KW, Machado AW, Moon W. The effects of micro-implant assisted rapid palatal expansion (MARPE) on the nasomaxillary complex. A finite element method (FEM) analysis. *Prog Orthod* 2014;15:52.
23. Park JJ, Park YC, Lee KJ, Cha JY, Tahk JH, Choi YJ. Skeletal and dentoalveolar changes after miniscrew-assisted rapid palatal expansion in young adults: A cone-beam computed tomography study. *Korean J Orthod* 2017;47:77-86.
24. Pereira MD, Prado GP, Abramoff MM, *et al.* Classification of midpalatal suture opening after surgically assisted rapid maxillary expansion using computed tomography. *Oral Surg Oral Med Oral Pathol Oral Radiol Endod* 2010;110:41-45.
25. Persson M, Thilander B. Palatal suture closure in man from 15-35 years of age. *Am J Orthod* 1977;72:42-52.
26. Pirelli P, Saponara M, Guilleminault C. Rapid maxillary expansion in children with obstructive sleep apnea syndrome. *Sleep* 2004;27:761-766.
27. Proctor DF, Anderson I. The nose: upper airway physiology and the atmospheric environment. Amsterdam: Elsevier Biomedical Press, 1985.
28. Quo SD, Hyunh N, Guilleminault C. Bimaxillary expansion therapy for pediatric sleep-disordered breathing. *Sleep Medicine* 2017;30:45-51.
29. Seong EH, Choi SH, Kim HJ, Yu HS, Park YC, Lee KJ. Evaluation of the effects of miniscrew incorporation in palatal expanders for young adults using finite element analysis. *Korean J Orthod* 2018;48:81-89.
30. Shetty V, Caridad JM, Caputo AA, *et al.* Biomechanical rationale for surgical-orthodontic expansion of the adult maxilla. *J Oral Maxillofac Surg* 1994;52:742-749.
31. Villa MP, Rizzoli A, Miano S, *et al.* Efficacy of rapid maxillary expansion in children with obstructive sleep apnea syndrome: 36 months of follow-up. *Sleep Breath* 2011;15:179-184.
32. Vinha PP, Eckeli AL, Faria AC, Xavier SP, de Mello-Filho FV. Effects of surgically assisted rapid maxillary expansion on obstructive sleep apnea and daytime sleepiness. *Sleep Breath* 2016;20:501-508.
33. Williams BJ, Currimbhoy S, Silva A, *et al.* Complications following surgically assisted rapid palatal expansion: a retrospective cohort study. *J Oral Maxillofac Surg* 2012;70:2394-2402.
34. Wootton DM, Luo H, Persak SC, *et al.* Computational fluid dynamics endpoints to characterize obstructive sleep apnea syndrome in children. *J Appl Physiol* 2014;116:104-112.
35. Yoon A, Guilleminault C, Zaghi S, Liu SY. Distraction osteogenesis maxillary expansion (DOME) for adult obstructive sleep apnea patients with narrow maxilla and nasal floor. *Sleep Med* 2020;65:172-176.